Test on the parameter dependence of coronal heating models

P. Démoulin[1], C.H. Mandrini[2], J.A. Klimchuk[3]

[1] Observatoire de Paris, section Meudon, DASOP, UMR 8645 (CNRS), F-92195 Meudon Principal Cedex, France
[2] Instituto de Astronomía y Física del Espacio, IAFE, CC. 67 Suc. 28, 1428 Buenos Aires, Argentina
[3] Naval Research Laboratory, Code 7675, Washington DC 20375-5352, USA

Abstract. The motivation of this work has been to provide observational constraints on coronal heating models by testing their predictions for the heating rate as a function of several physical parameters.
In Mandrini et al. (1999), we have investigated how the magnetic field strength, $< B >$, of coronal flux tubes depends on the end-to-end length, L, of the tube. For flux tubes of intermediate length, $50 \leq L \leq 300$ Mm, corresponding to the soft X-ray loops in a study by Klimchuk & Porter (1995), we find a universal scaling law of the form $< B > \propto L^{\delta}$, where $\delta = -0.88 \pm 0.3$. By combining this with the Klimchuk & Porter result that the heating rate scales as L^{-2}, we can test different models of coronal heating. We find that models involving the gradual stressing of the magnetic field, by slow footpoint motions, are in generally better agreement with the observational constraints than are wave heating models.

1. Introduction

Since it was realized that the solar corona is two orders of magnitude hotter than the underlying photosphere, scientists have puzzled over the reason for these extreme conditions. A number of plausible ideas to characterize the physical mechanism have been proposed, including the dissipation of stressed, current-carrying magnetic fields or the dissipation of MHD waves. Recognizing that loops are the fundamental building blocks of the corona, Klimchuk & Porter (1995) attacked the coronal heating problem by determining scaling laws for loops observed by the Soft X-ray Telescope (SXT) aboard *Yohkoh* (see also Porter & Klimchuk, 1995). They found that loop temperature and length are statistically uncorrelated and that pressure varies inversely with length to approximately the first power. Since the lifetimes of the loops are much longer than their cooling times, the authors used quasistatic loop equilibrium theory to infer that the volumetric heating rate scales inversely with length to approximately the second power. This is an important result, since different coronal heating models make different predictions about what the scaling between heating rate and length should be. Klimchuk & Porter were unable to make definitive tests, however, because the model predictions depend upon the statistical relationship that exists between field strength and loop length, and this was unknown at the time of their study. All that could be said was that models are consistent with the SXT observations only if $B \propto L^{\delta}$, where B is the field strength, L is the length, and the power-law index δ is model dependent.

In order to test different models of coronal heating, Mandrini et al. (1999) have investigated how the magnetic field strength of coronal flux tubes depends on the end-to-end length of the tube. Using photospheric magnetograms from both observed and idealized active regions, we computed potential, linear force-free, and magnetostatic extrapolation models. For each model, we then determined the average coronal field strength, $< B >$, in approximately one thousand individual flux tubes with regularly spaced footpoints. Scatter plots of $< B >$ versus length, L, are characterized by a flat section for small L and a steeply declining section for large L. They are well described by a function of the form $< B >= C_1 + C_2 \ \log L + C_3/2 \ \log(L^2 + S^2)$, where $C_2 \approx 0$, $-3 \leq C_3 \leq -1$, and $40 \leq S \leq 240$ Mm is related to the characteristic size of the active region. There is a tendency for the magnitude of C_3 to decrease as the magnetic complexity of the region increases. For flux tubes of intermediate length, $50 \leq L \leq 300$ Mm, corresponding to the soft X-ray loops in a study by Klimchuk & Porter (1995), we find a universal scaling law of the form $< B > \propto L^{\delta}$, where $\delta = -0.88 \pm 0.3$.

Here, our goals are to combine the above result with the Klimchuk & Porter result that the heating rate scales as L^{-2}, in order to test different models of coronal heating.

2. An overview on coronal heating models

Models or theories of coronal heating can be divided into two main categories: stressing models, in which energy is extracted from coronal magnetic fields that are stressed by slow footpoint motions, and wave models, in which energy is deposited by waves that are incident from below. These are also sometimes referred to as direct current (DC) and alternating current (AC) models, respectively. Many models address the question of how the free magnetic energy or wave energy is dissipated, while others are concerned only with the origin of this energy and do not prescribe a specific dissipation mechanism. We now describe briefly a number of different models, first considering those in the stressing category and then considering those in the wave category. The models are listed in Table 1

	N^0	References	Scaling law	Parameters
Stressing Models (DC)				
Stochastic buildup	1	Sturrock & Uchida 1981,	$B^2L^{-2}V^2\tau$	
–		Berger 1991		
Critical angle	2	Parker 1988,	$B^2L^{-1}V\tan\theta$	
–		Berger 1993		
Critical twist	3	Galsgaard & Nordlund 1997	$B^2L^{-2}VR\phi$	
Reconnection $\propto v_A$	4	Parker 1983	$BL^{-2}\rho^{1/2}V^2R$	
Reconnection $\propto v_{A\perp}$	5	Parker 1983, modified	$B^{3/2}L^{-3/2}\rho^{1/4}V^{3/2}R^{1/2}$	
Current layers	6	van Ballegooijen 1986	$B^2L^{-2}V^2\tau\log R_m$	
–	7	Hendrix et al. 1996	$B^2L^{-2}V^2\tau\mathrm{S}^{0.1}$	
–	8	Galsgaard & Nordlund 1996	$B^2L^{-2}V^2\tau$	
Current sheets	9	Aly & Amari 1997	$B^2L^{-1}V_{ph}^2\tau$	
Taylor relaxation	10	Heyvaerts & Priest 1984, Browning & Priest 1986, Vekstein et al. 1993	$B^2L^{-2}V_{ph}^2\tau$	
Turbulence with:				
Constant dissipation coefficients	11	Einaudi et al. 1996, Dmitruk & Gómez 1997	$B^{3/2}L^{-3/2}\rho^{1/4}V^{3/2}\mathrm{R}^{1/2}$	
Closure	12	Heyvaerts & Priest 1992, Inverarity et al. 1995, Inverarity & Priest 1995a	$B^{5/3}L^{-4/3}\rho^{1/6}V^{4/3}\mathrm{R}^{1/3}$	
Closure + spectrum	13	Milano et al. 1997	$B^{s+1}L^{-1-s}\rho^{(1-s)/2}V^{2-s}\mathrm{R}^s$	$s = 0.7, m = -1.$
	14			$s = 1.1, m = -2.5$
Wave Models (AC)				
Resonance	15	Hollweg 1985	$B^{1+m}L^{-3-m}\rho^{-(1+m)/2}$	$m = -1.$
–	16			$m = -2.$
Resonant absorption	17	Ofman et al. 1995,	$B^{1+m}L^{-1-m}\rho^{-(1+m)/2}$	$m = -1.$
–	18	Ruderman et al. 1997		$m = -2.$
–	19	Halberstadt &	$B^{1+m}L^{-m}\rho^{-(m-1)/2}$	$m = -1.$
–	20	Goedbloed 1995		$m = -2.$
Current layers	21	Galsgaard & Nordlund 1996	$BL^{-1}\rho^{1/2}V^2$	
Turbulence	22	Inverarity & Priest 1995b	$B^{5/3}L^{-4/3}\mathrm{R}^{1/3}$	

Table 1: Summary of the scaling law for different models of coronal heating.

together with the scaling laws that they predict. The parameters included in these laws are defined either in this section or in §3. We note that the parameter R that appears in many of the scaling laws cannot always be interpreted straightforwardly as the loop radius (See the discussion in Mandrini et al., 1999).

2.1. Stressing models

Photospheric and subphotospheric motions displace magnetic footpoints in both random and systematic ways and can include both translational and rotational components. The magnetic free energy that is pumped into the field can be released in real time or stored in the field to be released later. Thus, the resulting plasma heating can be steady, quasi-steady, or highly episodic, depending on the model. Quasi-steady heating refers to situations where the time interval between heating events is short compared to the cooling time by radiation and thermal conduction.

Stochastic Buildup. Model 1 (Sturrock & Uchida 1981; Berger 1991) considers the random twisting of individual flux tubes. The energy grows linearly with time, on average, and is assumed to dissipate episodically at intervals that are long compared with the correlation time of the flow. The heating events can be large or small, and can eliminate all or part of the twist. This scaling law also applies to stochastic energy buildup resulting from random translation motions.

Critical Angle. When the random walk step size is not short compared to the correlation length, the field becomes entangled and braided, and the energy builds quadratically with time in a monotonic fashion. This is the scenario in model 2 (Parker 1988; Berger 1993), which supposes that heating occurs when a critical angle θ is reached between adjacent misaligned flux tubes. Parker suggests that a steady state is set up in which dissipation balances energy input to maintain the angle at or close to the critical value. In fact, the same scaling law applies even if the heating is highly episodic and the angle decreases substantially between events.

Critical Twist. Model 3 (Galsgaard & Nordlund 1997) is similar, except that energy release occurs when a flux tube reaches a critical twist angle, ϕ, perhaps due to the onset of a kink instability. Note that ϕ is the end-to-end angular rotation of the twisted tube, which is different from θ.

Reconnection. Magnetic reconnection may be responsible for the conversion of magnetic to thermal energy in the above models, but this is not explicitly treated. In model 4 (Parker 1983), it is the prescribed mechanism. It is assumed to occur at tangential discontinuities (current sheets) that are postulated to form even in simple magnetic configurations when footpoints are displaced by continuous motions. The scaling law is derived by equating the magnetic reconnection rate with the energy buildup rate. If we modify Parker's original derivation to account for the fact that the reconnection rate is likely to depend on the transverse field strength, rather than the total field strength, we obtain model 5, with a somewhat different scaling law.

Current Layers. There is considerable skepticism that current sheets will actually form from continuous footpoint motions unless the coronal magnetic field is sufficiently complex (contains nulls, separatrices, etc.). Nonetheless, there is widespread agreement that currents can easily become concentrated in layers of small but finite thickness. In model 6 (van Ballegooijen 1986), energy that is pumped into the field over large scales gradually goes to smaller and smaller scales until eventually the scale is small enough for Ohmic dissipation to be effective. Models 7 (Hendrix et al. 1996) and 8 (Galsgaard & Nordlund 1996) are fundamentally similar to model 6, except that they involve MHD simulations. Simple footpoint shearing motions are imposed at the boundary with the direction of motion rotating by 90^0 at time intervals selected randomly. Currents develop exponentially at stagnation points in the corona, but they are dissipated rather suddenly after growing for only about one correlation time of the driver. No significant braiding occurs.

Current Sheets. Model 9 (Aly & Amari 1997) considers the formation and destruction of true current sheets in magnetic configurations containing X-points. Such sheets appear and grow naturally from X-points in the presence of a steady flow. It is proposed that these sheets dissipate episodically, by magnetic reconnection, in a sequence of energy release events.

Taylor Relaxation. Model 10 (Heyvaerts & Priest 1984; Browning & Priest 1986; Vekstein, Priest & Steele 1993) makes use of Taylor's well known conjecture (1974) that magnetic fields relax via reconnection to the lowest energy state that conserves helicity—the linear force-free state. In this scenario, footpoint motions produce nonlinear force-free fields, and these fields episodically relax to the corresponding linear field having the same helicity, thereby releasing energy.

Turbulence. Turbulence may develop in the corona, where the Lundquist number exceeds the critical threshold by many orders of magnitude. Two different approaches have been used to study turbulent heating in the corona. Model 11 (Einaudi et al. 1996; Dmitruk & Gómez 1997) involves MHD simulations in a two-dimensional plane corresponding to a cross-sectional cut across a flux tube. The coefficients of resistivity and kinematic viscosity are constant and, for computational reasons, much larger than actual coronal values. Turbulence develops as part of the time-dependent solution and is not assumed *a priori*. Models 12 (Heyvaerts & Priest 1992; Inverarity, Priest & Heyvaerts 1995; Inverarity & Priest 1995a) and 13 (Milano, Gómez & Martens 1997) are fully three dimensional, but the nonlinear terms in the Equations are replaced by diffusion terms which mimic the effects of an assumed turbulence. The turbulent diffusion coefficients are free parameters and are determined self-consistently according to "closure models" that relate the magnitudes of the coefficients to the magnitude of the energy cascade and, hence, the magnitude of the energy input by footpoint driver motions. These motions are assumed to have a Kolmogorov spectrum in wavenumber ($\propto k^{-5/3}$), and model 13 also includes a power-law spectrum in frequency ($\propto \omega^m$). The parameter s in the scaling law is related to m as indicated in the last column of Table 1.

2.2. Wave models

Waves occur in coronal loops whenever the time scale of the motions is shorter than the end-to-end Alfvén travel time. Although waves can be generated directly in the corona, such as by bursty reconnection, we do not consider that situation here since the energy that powers the waves resides initially in the stressed coronal magnetic fields. We instead concentrate on models in which the waves are generated at the base of the corona, possibly by photospheric turbulence, and propagate upward to heat the corona.

Resonance. Because of the steep density and temperature gradients at the footpoints of coronal loops, wave energy can be both reflected and transmitted at the boundary. The loop acts as a driven, leaky, resonance cavity. Model 15 (Hollweg 1985) addresses the conditions that must be met in order for significant energy to be transmitted into the loop from below. The scaling law for this model depends on the power law index of the assumed driver frequency spectrum, m.

Resonant Absorption. Models 17–20 (Ofman, Davila & Steinolfson 1995; Ruderman et al. 1997; Halberstadt & Goedbloed 1995) consider a different aspect of loop resonance. Whenever the Alfvén velocity is nonuniform in a loop cross-section a phenomenon know as resonant absorption occurs. The wave amplitude is enormously enhanced in a narrow layer where the local Alfvén resonance frequency matches the frequency of the global loop oscillations. Gradients in the magnetic field and velocity are extremely large in this layer, and the wave energy is easily dissipated by Ohmic and viscous processes.

Current Layers. Model 21 (Galsgaard & Nordlund 1996) is basically the same model as model 8 but taken in the limit of rapid boundary excitations compared to the the end-to-end Alfvén travel time. Compared to previous wave models, one major difference is that the boundary condition is not described by a power-law spectrum in frequency, but rather by a series of shearing motions randomly modified.

Turbulence. Model 22 (Inverarity & Priest 1995b) is similar to model 12 except that the footpoint motions have a high enough frequency to produce waves rather than a quasistatic evolution.

3. How can observations test heating models?

The aim of coronal-heating models is to identify the mechanism responsible for the energy input at coronal heights. However, many of the hypotheses involved (e.g. the formation of small scale lengths) are not directly verifiable with present observations. One test that is typically applied to models is to compare the predicted heating rate with that obtained from observations. Several models pass this test successfully for both quiet Sun and active region conditions. The aim of our work is, finally, to provide more severe constrains by comparing the dependence given by models with those deduced from observations.

As shown in Table 1, most coronal heating models give a heating rate per unit volume which can be expressed in the following generic way:

$$H_m \propto B^a L^b \rho^c V^d R^e \,, \tag{1}$$

where B and ρ are the coronal field strength and plasma density, L is the loop length, V is the transverse velocity at the base of the corona, and R is the loop radius (for most models).

If B, ρ, V, and R have a known power-law dependence on L, Equation 1 reduces to the simple form

$$H_m \propto L^{\alpha_m} \,, \tag{2}$$

where the "m" subscript indicates a model quantity. This can be compared to the observed relationship

$$H \propto L^{\alpha} \tag{3}$$

determined from *Yohkoh* data by Porter & Klimchuk 1995. If α_m and α agree to within the uncertainties, then the model can be considered viable. Otherwise, it must be rejected. Porter & Klimchuk obtained independent estimates of α based the the observed relationships $P \propto L^{\beta}$ and $T \propto L^{\gamma}$. The pressure scaling gives a most probable value for α of -1.95 with a 90% confidence interval of [-3.11, -0.95], while the temperature scaling gives -2.00 and [-4.59, -0.67]. Note that the most probable values are essentially identical, and in §4. we refer to a single result.

3.1. Effects of boundary conditions

The quantities V and R in Eq.(1) refer to the base of the corona, which is separated from the photosphere by the chromosphere and transition region. On the other hand, the driver motions which displace the coronal magnetic field are associated with convection, or some other turbulent or organized flows that originate at or below the photosphere. How are V and R related in these two regions? One possibility, which we refer to as Case (a), is that the coronal and photospheric quantities are identical:

$$R = R_{ph} \, , V = V_{ph} \qquad \text{(Case (a))} \, . \tag{4}$$

This is the assumption made for nearly all published models.

A second possibility, Case (b), takes into account the well-known fact that the photospheric field is strongly concentrated in thin flux tubes. Magnetic flux conservation implies:

$$R \approx R_{ph} \sqrt{\frac{B_{ph}}{B}} \qquad \text{(Case (b))} \, . \tag{5}$$

Any braiding or shearing motions in the photosphere are transmitted to the bottom of corona with nearly the same amplitude. However, the velocity of twisting motions will be amplified due to the flux tube expansion (van Ballegooijen 1986). For a stationary twisting motion, the twisting velocity at the base of the corona is:

$$V \approx V_{ph} \sqrt{\frac{B_{ph}}{B}} \qquad \text{(Case (b))} \, . \tag{6}$$

Because plasma densities are so much larger in the photosphere than in the corona, it is reasonable to suppose that photospheric quantities are essentially unaffected by the physical conditions of the corona. This suggests that B_{ph}, R_{ph}, and V_{ph} are statistically independent of the coronal loop length, L. With this hypothesis, the power-law index in Eq.(2) has the form α_m given by:

$$\alpha_m = \delta a + b + \epsilon c \qquad \text{for Case (a)} \, , \tag{7}$$

and

$$\alpha_m = \delta(a - (d+e)/2) + b + \epsilon c \qquad \text{for Case (b)} \, , \tag{8}$$

where we have assumed that other parameters intrinsic to some of the models, are also statistically independent of the loop length L.

4. Test on the heating models

Fig.1 shows the values of α_m predicted by the different models in Table 1. The derivation of the error bars is explained in Mandrini et al (1999). The horizontal line in Fig.1 indicates the observed value, α, determined by Porter & Klimchuk. The shaded bands

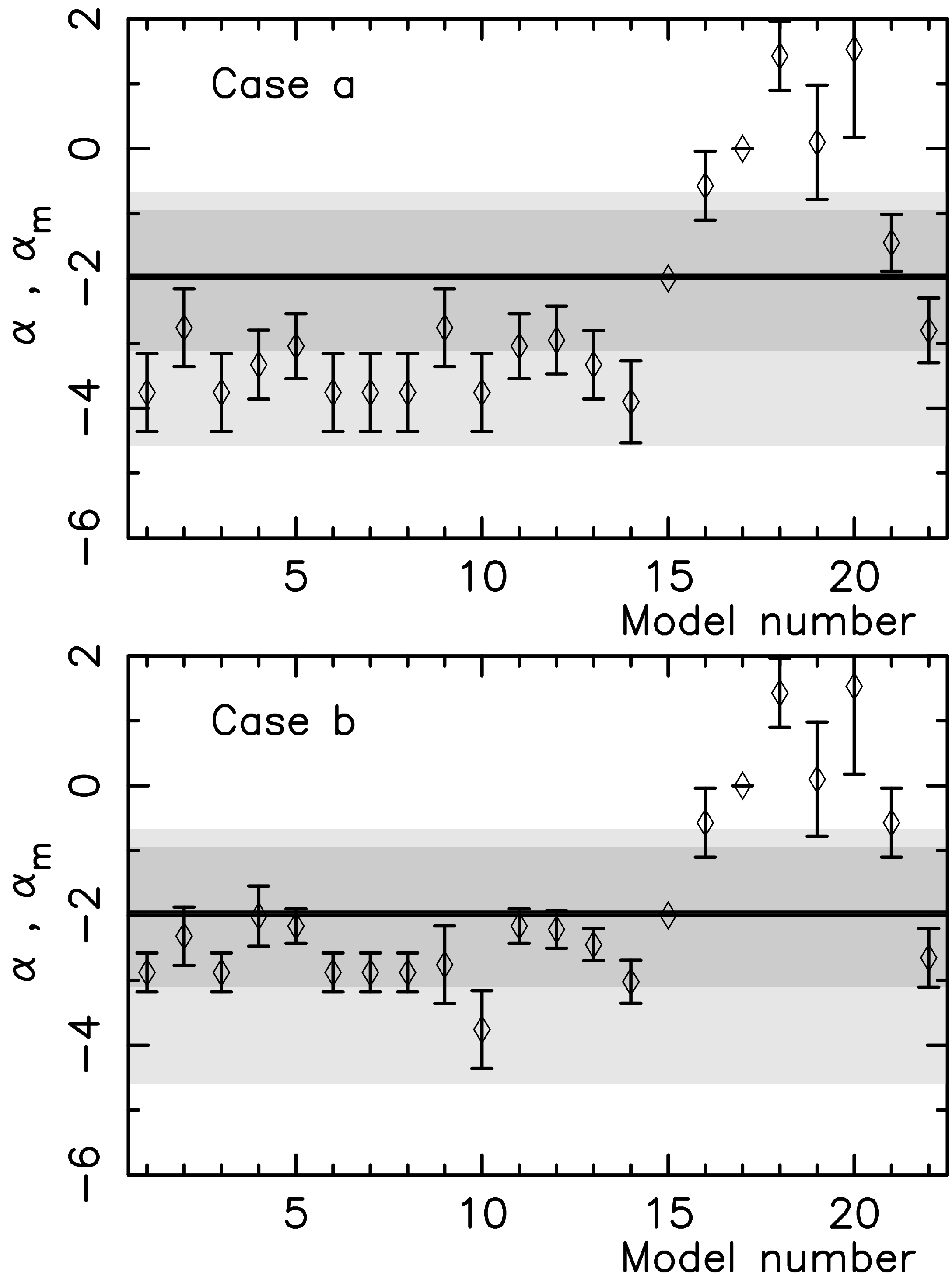

Figure 1: Comparison of the heating rate versus length scaling law, $H \propto L^{\alpha}$, as deduced from observations and models. The plotted points with error bars indicate the power-law index α_m predicted by the models listed in Table 1. The horizontal line at $\alpha = -2$ is the most probable value deduced from observations (Porter & Klimchuk, 1995), with the dark (resp. light) shaded band representing the 90% confidence interval associated with the pressure (resp. temperature) measurements.

indicate the 90% confidence intervals determined with the pressure scaling (dark, narrow band) and the temperature scaling (light, broad band). In order for a model to be strictly consistent with the *Yohkoh* observations, its error bar must overlap with the dark band. Only some of the models satisfy this requirement. However, in all but models 17–20, the disagreement is quite small, and given the approximate nature of the error estimations, it is not appropriate to reject these models as impossible.

We nonetheless find that some models are in better agreement with the observations than others. In particular, with the hypothesis of no flux expansion (Case (a)), models in which energy release occurs at a critical angle of the magnetic field (Parker 1988; Berger 1993; model 2) or which involve magnetic reconnection (Parker 1983; models 4 and 5; Aly & Amari 1997; model 9) or which involve turbulence (Einaudi et al. 1996; Dmitruk & Gómez 1997; Heyvaerts & Priest 1992; Inverarity, Priest & Heyvaerts 1995; Inverarity & Priest 1995a; models 11 and 12) predict α_m very close to the most probable value. Wave heating models, especially models 17-20, exhibit the poorest agreement with these observations with the remarkable exception of model 15 (Hollweg 1985) while models 21 and 22 (Galsgaard & Nordlund 1996; Inverarity & Priest 1995b) are both close to the most probable value of α.

Taking into account the magnetic flux expansion (Case (b)), nearly all the stressing models (except model 10 which involves Taylor relaxation) are closer to the most probable value determined by Porter & Klimchuk. This is a warning that flux-tube expansion should be treated in models (rather than the often used uniform field).

Acknowledgements

We thank Drs. Giorgio Einaudi, Daniel Gómez, Joe Hollweg, Leon Ofman, Grigory Vekstein, and Marco Velli for helpful discussions on their models. P.D. and C.H.M. acknowledge financial support from ECOS (France) and SECYT (Argentina) through their cooperative science program (A97U01). The work of J.A.K. was supported by NASA contract W-19,200.

References

Aly, J.J. & Amari, T. 1997, A&A, 319, 699

Berger, M.A. 1991, A&A, 252, 369

Berger, M.A. 1993, Phys. Rev. Lett., 70, 705

Browning, P.K. & Priest, E.R. 1986, A&A, 159, 129

Dmitruk, P. & Gómez, D.O., 1997, ApJ, 484, L83

Einaudi, G., Velli, M., Politano, H. & Pouquet, A. 1996, ApJ, 457, L113

Galsgaard, K. & Nordlund, A. 1996, JGR, 101, A6, 13445

Galsgaard, K. & Nordlund, A. 1997, JGR, 102, A1, 219

Halberstadt, G. & Goedbloed, J.P. 1995, A&A, 301, 559

Hendrix, D.L., Van Hoven, G., Mikić, Z. & Schnack, D.D. 1996, ApJ, 470, 1192

Heyvaerts, J. & Priest, E.R. 1984, A&A, 137, 63

Heyvaerts, J. & Priest, E.R. 1992, ApJ, 390, 297

Hollweg, J.V. 1985, in Adv. in Space Plasma Physics, ed. B. Buti (Singapore: World Scientific Pub. Co.), 77

Inverarity, G.W., Priest, E.R. & Heyvaerts, J. 1995, A&A, 293, 913

Inverarity, G.W. & Priest, E.R. 1995a, A&A, 296, 395

Inverarity, G.W. & Priest, E.R. 1995b, A&A, 302, 567

Klimchuk, J. A., & Porter, L. J. 1995, Nature, 377, 131

Mandrini, C.H., Démoulin, P., Klimchuk J.A., ApJ, 1999, in press

Milano, L.J., Gómez, D.O., Martens, P.C.H. 1997, ApJ, 490, 442

Ofman L., Davila, J.M. & Steinolfson R.S. 1995, ApJ, 444, 471

Parker, E.N. 1983, ApJ, 264, 642

Parker, E.N. 1988, ApJ, 330, 474

Parker, E.N. 1994, Spontaneous Current Sheets in Magnetic Fields, Oxford University Press, Oxford

Porter, L.J. & Klimchuk, J.A. 1995, ApJ, 454, 499

Ruderman, M.S., Berghmans, D., Goosens, M. & Poedts, S. 1997, A&A, 320, 305

Sturrock, P.A. & Uchida, Y. 1981, ApJ, 246, 331

van Ballegooijen, A.A. 1986, ApJ, 311, 1001

Vekstein, G.E., Priest, E.R. & Steele, C.D.C. 1993, ApJ, 417, 781

Discussion

S. Antiochos: How about the absolute magnitude of the heating as predicted by the models? Is that sufficient to explain the observed heating losses in coronal loops?

P. Démoulin: Most models in table I give easily the right order of energy input in the corona when using standart values of the solar atmosphere (others have been eliminated as possible explanation of the coronal heating, e.g. acoustic waves). However some models give a heating which is smaller than observed, e.g. a factor around 40 too low in the case of model 6 (van Ballegooijen 1986). For the wave models 15–20, there is a large uncertainty on the power law index m. With a flat spectrum ($m \approx 0$), there is enough power in the high frequency waves to heat the corona, but the index is likely to be negative (e.g. $m = -1$ for a Kolmogoroff photospheric spectrum) and, in this case, there is not enough available energy at the coronal loop resonance (see e.g. Parker, 1994, section 11.4). Finally, presently data are not precise enough to eliminate models in table I just on the magnitude of the coronal heating produced (an order of magnitude can be easily gained by shifting the parameters within the error bars).